iScience, Volume *23*

Supplemental Information

A Major Change in Rate of Climate Niche Envelope Evolution during Hominid History

Alessandro Mondanaro, Marina Melchionna, Mirko Di Febbraro, Silvia Castiglione, Philip B. Holden, Neil R. Edwards, Francesco Carotenuto, Luigi Maiorano, Maria Modafferi, Carmela Serio, Josè A.F. Diniz-Filho, Thiago Rangel, Lorenzo Rook, Paul O'Higgins, Penny Spikins, Antonio Profico, and Pasquale Raia

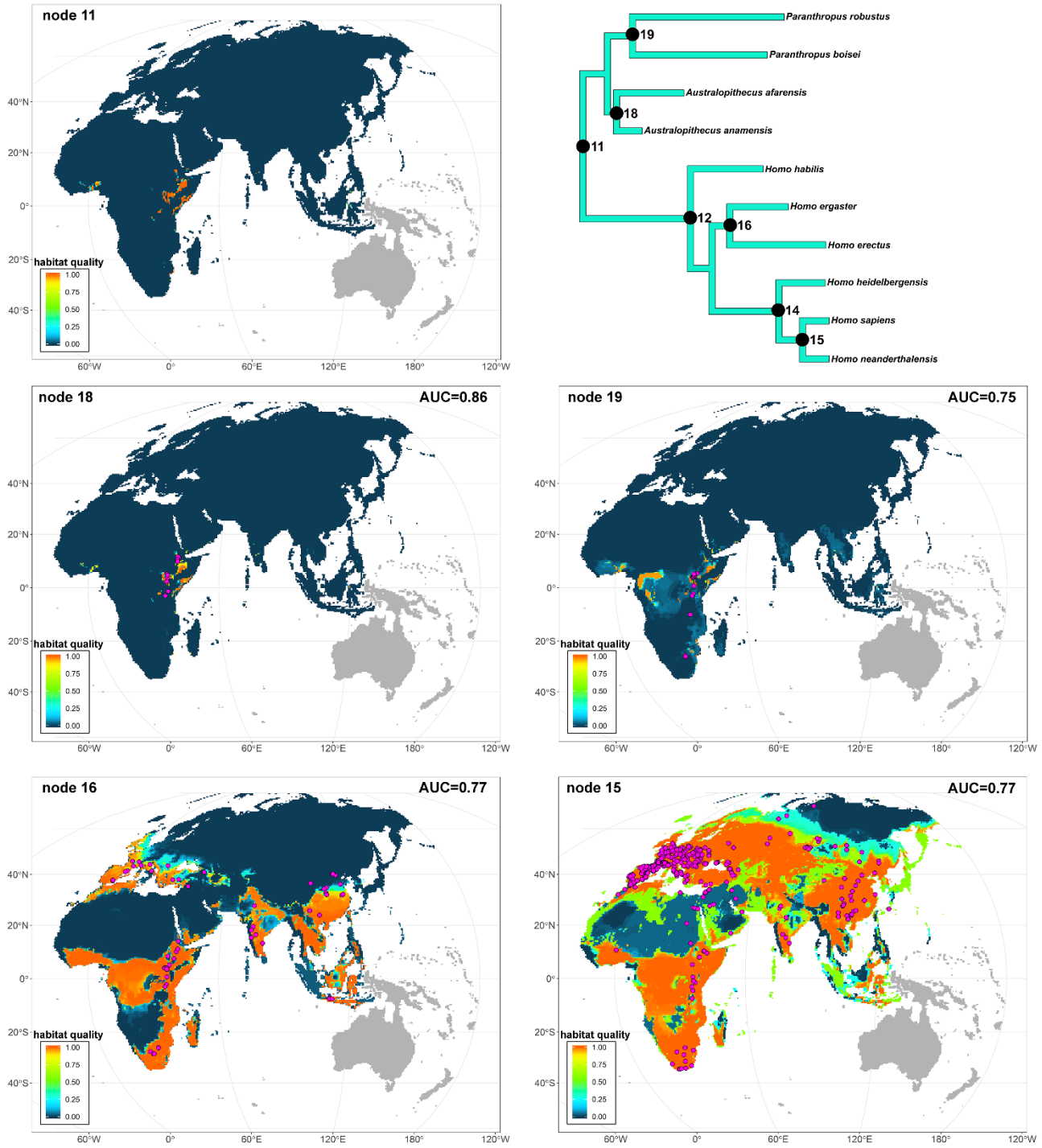

Figure S1. Maps of fossil locality distribution and habitat quality at specific nodes in the hominin tree. Related to Figures 1 and 2.

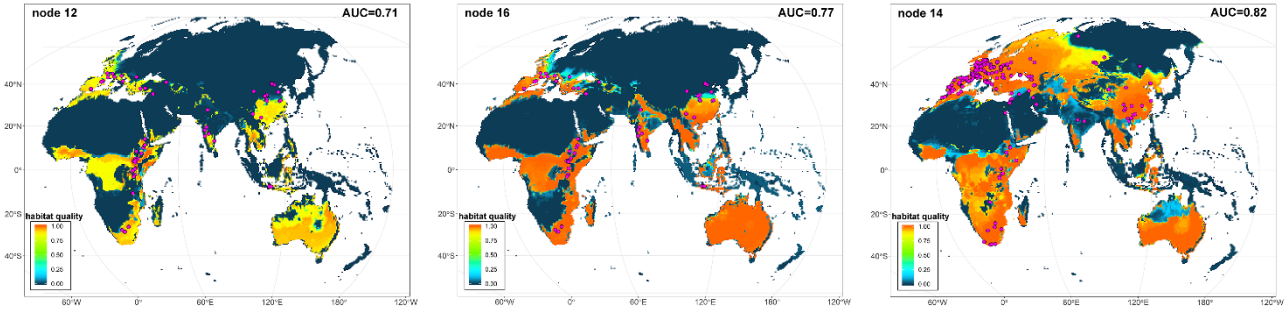

Figure S2. Maps of fossil locality distribution and habitat quality at specific nodes in the hominin tree, after setting the maximum number of fossil localities per species at 100 for the ancestor to all *Homo* species (node 12, left), early *Homo* (node 16, middle) and MHS (node 14, right). Related to Figures 1 and 2.

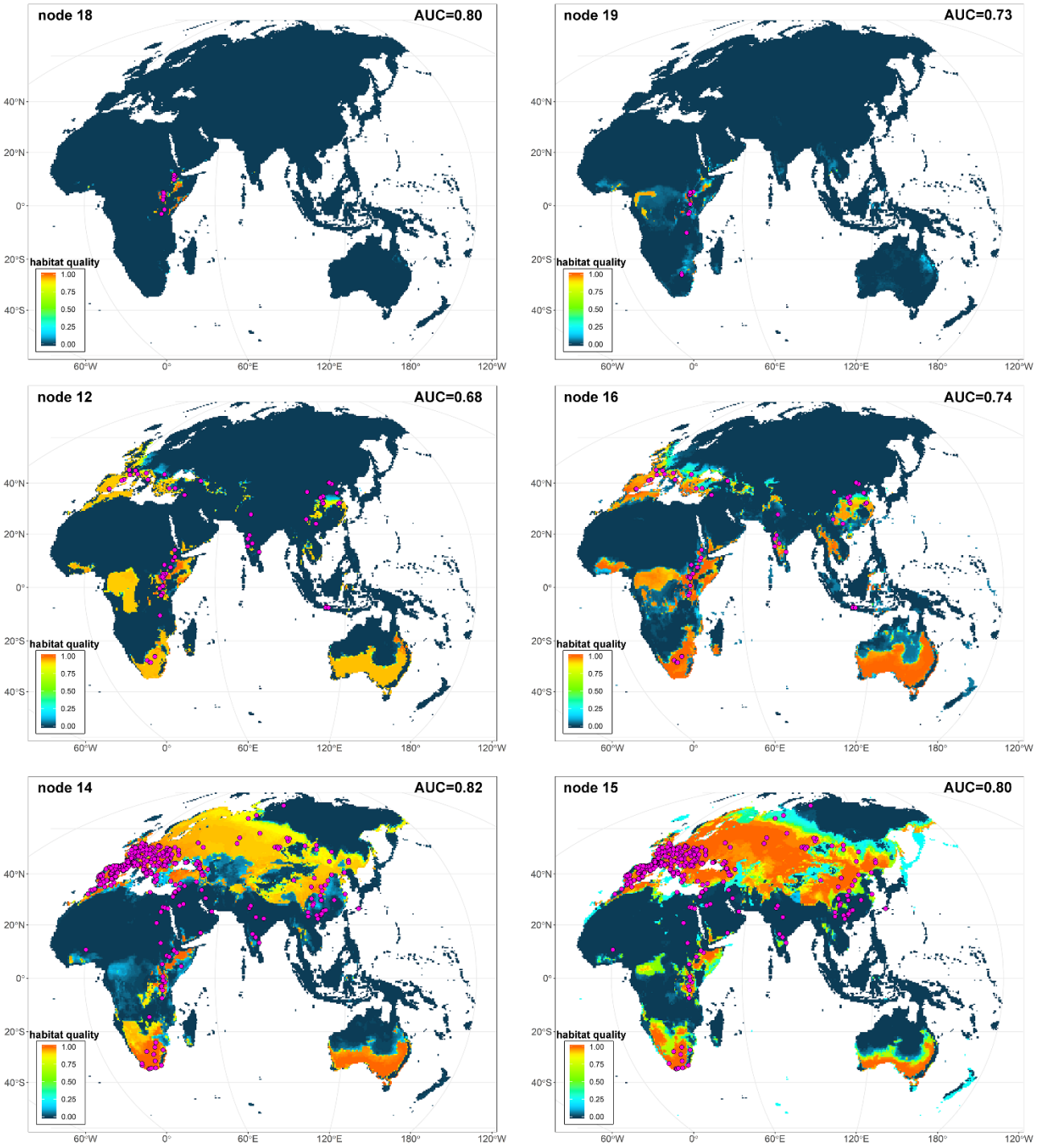

Figure S3. Maps of fossil locality distribution and habitat quality at specific nodes in the hominin tree, after excluding the first decile of the distribution of paleoclimatic estimates. The node numbers correspond to the tree in Figure S1. Related to Figures 1 and 2.

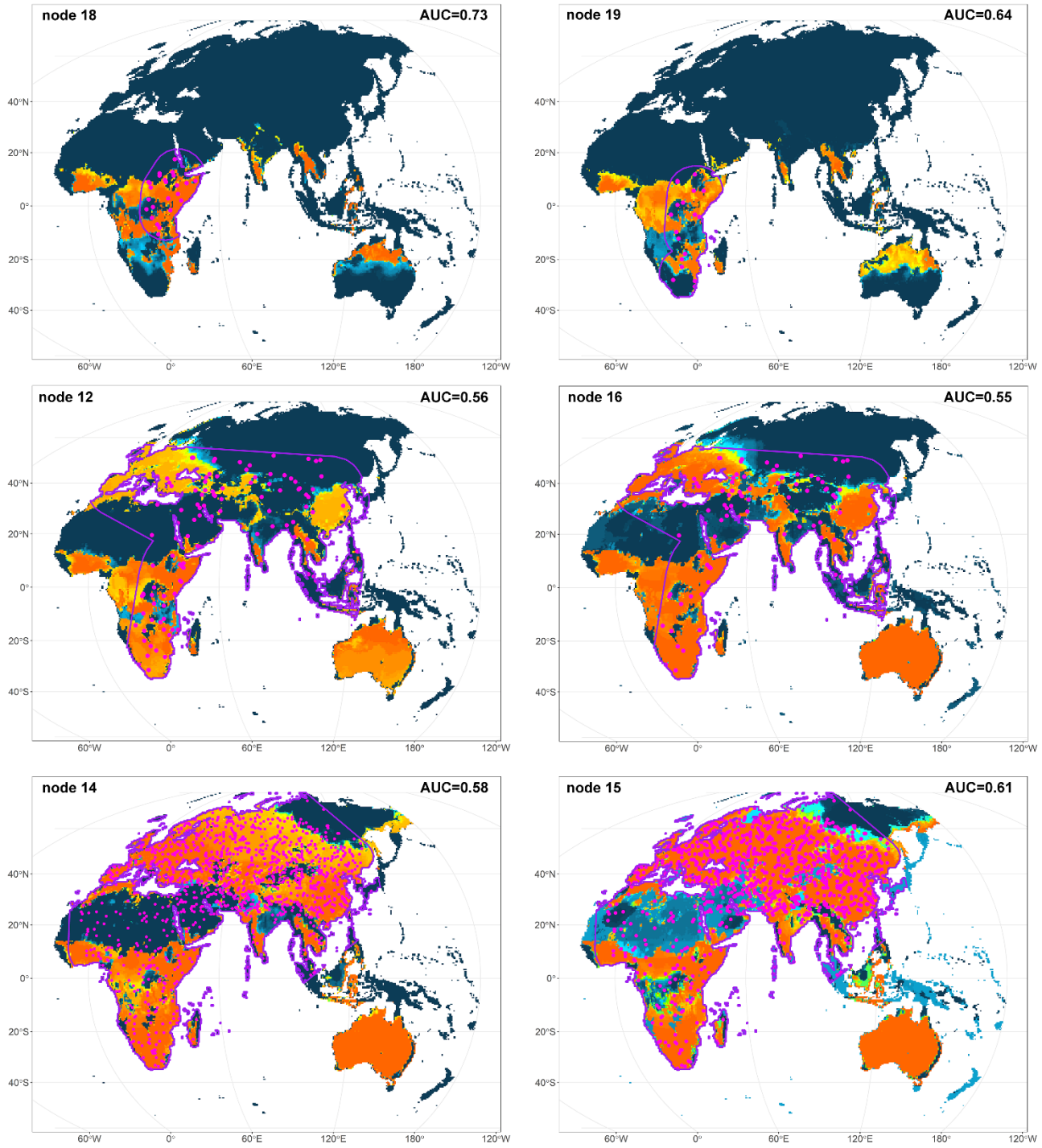

Figure S4. Maps showing randomly placed fossil localities and habitat quality at specific nodes in the hominin tree. Related to Figures 1 and 2.

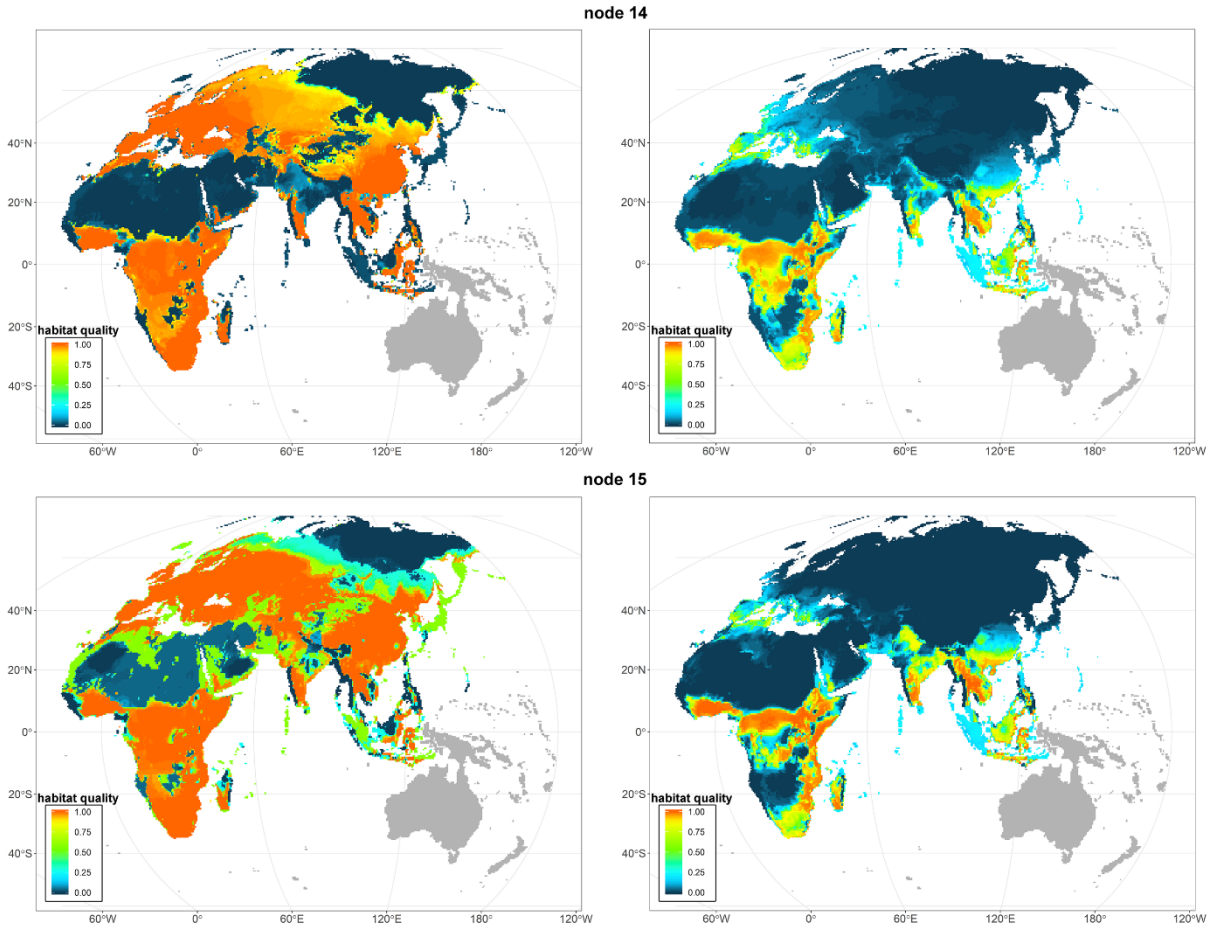

Figure S5. Maps of habitat quality estimated for the ancestors of MHS (node 14 in the tree) and the ancestor of *H. sapiens* plus *H. neanderthalensis* (node 15). Related to Figures 1 and 2.

A

Species	minPrec (mm)	minTemp (°C)	Min NPP	maxPrec (mm)	maxTemp (°C)	Max NPP	extinction age (Ma)
Australopithecus anamensis	8.5	16.7	73.7	561.7	30.4	699.3	3.85
Australopithecus afarensis	13.4	22.0	48.3	465.3	29.8	431.3	3.00
Paranthropus boisei	0.6	-15.5	0.0	2000.0	31.2	909.3	1.30
Paranthropus robustus	6.0	9.4	0.2	1094.2	33.2	981.9	0.96
Homo habilis	7.7	13.9	22.6	782.6	30.8	848.8	1.39
Homo ergaster	0.0	-12.3	0.0	963.3	30.2	1113.7	0.88
Homo erectus	0.0	-28.2	0.0	586.1	29.2	1093.4	0.11
Homo heidelbergensis	0.0	-33.6	0.0	1105.5	35.6	1458.0	0.20
Homo neanderthalensis	5.7	16.6	58.9	877.6	29.6	852.4	0.04
Homo sapiens	14.2	9.8	333.9	339.9	24.0	456.6	0.04

B

Node	descendants	minPrec	minTemp (°C)	Min NPP	maxPrec (mm)	maxTemp (°C)	Max NPP	mean age (Ma)
11	hominins	12.5	20.0	52.6	513.0	29.9	490.8	4.96
12	*Homo* spp.	6.0	3.8	15.3	946.7	31.5	894.0	2.92
13	*Homo* spp. without *H. habilis*	4.8	0.0	8.8	1032.7	31.8	959.1	2.32
14	MHS	0.7	-21.1	1.7	904.8	31.7	1182.6	0.99
15	MHS without *H. heidelbergensis*	0.2	-23.7	0.5	878.8	31.5	1204.0	0.48
16	*H. ergaster* plus *H. erectus*	4.8	0.7	6.9	1080.7	31.9	960.1	1.91
17	australopiths	12.6	20.5	55.6	499.8	29.8	482.2	4.49
18	*Australopithecus* spp.	12.7	20.8	54.5	492.9	29.8	475.6	4.24
19	*Paranthropus* spp.	12.2	19.7	67.5	522.5	29.5	509.8	3.83

Table S1. A. Paleoclimatic estimates for the hominin species in the tree. B. Reconstructed climatic values at the tree nodes. Related to Figures 1 - 3.

A

Species	minPrec (mm)	minTemp (°C)	Min NPP	maxPrec (mm)	maxTemp (°C)	Max NPP	extinction age (Ma)
Australopithecus anamensis	13.5	22	48.3	465.3	29.8	431.3	3.85
Australopithecus afarensis	8.5	16.7	81.5	538.4	30.2	676.7	3
Paranthropus boisei	5.7	16.6	58.9	877.6	29.6	852.4	1.3
Paranthropus robustus	14.2	9.8	333.9	340	24	456.6	0.96
Homo habilis	7.7	13.9	22.6	782.56	30.8	848.8	1.39
Homo ergaster	6	9.4	0.2	1094.2	33.2	981.9	0.88
Homo erectus	0.6	-15.5	0	2000	31.2	909.3	0.11
Homo heidelbergensis	0	-10.6	0	878.5	29.4	1016.3	0.2
Homo neanderthalensis	0	-25.5	0	498.9	26	921.7	0.04
Homo sapiens	0	-29.6	0	952.9	32.8	922.8	0.04

B

Node	descendants	minPrec	minTemp (°C)	Min NPP	maxPrec (mm)	maxTemp (°C)	Max NPP	mean age (Ma)
11	hominins	12.4	20.3	53.4	510.4	29.8	490.9	4.96
12	*Homo* spp.	6	4.4	15.6	925.9	31	839.8	2.94
13	*Homo* spp. without *H. habilis*	4.8	0.7	9.2	1009.2	31.2	892.1	2.32
14	MHS	0.7	-18.6	1.6	809.1	29.6	945.3	0.98
15	MHS without *H. heidelbergensis*	0.2	-20.9	0.7	783.6	29.4	949.9	0.48
16	*H. ergaster* plus *H. erectus*	4.8	1.1	7.4	1060.8	31.5	904.1	1.92
17	australopiths	12.5	20.7	56.6	497.4	29.7	484.9	4.49
18	*Australopithecus* spp.	12.6	21.1	55.6	490.3	29.8	479.4	4.24
19	*Paranthropus* spp.	12.1	19.9	69.8	517.7	29.5	510.2	3.84

Table S2. A. Paleoclimatic estimates for the hominin species in the tree. B. Reconstructed climatic values at the tree nodes after subsampling the most abundant species. Related to Figures 1 - 3.

A

Species	minPrec (mm)	minTemp (°C)	Min NPP	maxPrec (mm)	maxTemp (°C)	Max NPP	extinction age (Ma)
Australopithecus anamensis	16	22.6	46.2	457.7	29.7	423.7	3.85
Australopithecus afarensis	10.5	17.1	76.7	490.6	29.8	625.7	3
Paranthropus boisei	5.1	15.7	54.4	657.8	29.4	648.7	1.3
Paranthropus robustus	13.9	8.4	330	332.5	23.6	446.9	0.96
Homo habilis	5.4	14.2	26.8	553.8	29.9	678.4	1.39
Homo ergaster	6.7	10	0.3	652.1	29.7	707.9	0.88
Homo erectus	0.6	-16.5	0	896.8	28.3	752.5	0.11
Homo heidelbergensis	5.4	14.2	26.8	553.8	29.9	678.4	0.2
Homo neanderthalensis	0	-17.3	0	380.6	24.9	706.5	0.04
Homo sapiens	0	-27.9	0	383.5	22.8	702.4	0.04

B

Node	descendants	minPrec	minTemp (°C)	Min NPP	maxPrec (mm)	maxTemp (°C)	Max NPP	mean age (Ma)
11	hominins	14.6	20.7	50.9	468.7	29.5	461	4.96
12	*Homo* spp.	5.8	3.1	15.1	579.1	28.7	658.8	2.89
13	*Homo* spp. without *H. habilis*	4.8	-0.1	10.3	594.3	28.5	679.2	2.33
14	MHS	0.9	-21.5	2.3	479.5	25.9	690.4	1.03
15	MHS without *H. heidelbergensis*	0.3	-24.9	1.1	458.6	25.5	692.5	0.48
16	*H. ergaster* plus *H. erectus*	4.9	0.6	7.8	617.5	28.7	687.2	1.89
17	australopiths	14.8	21.2	54	465.2	29.5	459.1	4.47
18	*Australopithecus* spp.	14.9	21.4	53.1	463.8	29.6	457.6	4.25
19	*Paranthropus* spp.	13.7	19.9	68.2	477.3	29.2	477.7	3.74

Table S3. A. Paleoclimatic estimates for the hominin species in the tree. B. Reconstructed climatic values at the tree nodes after removing the first decile of the climatic variable values. Nodes refer to the node number in the tree. Nodes refer to the node number in the tree. Related to Figures 1 - 3.

A

Species	minPrec (mm)	minTemp (°C)	Min NPP	maxPrec (mm)	maxTemp (°C)	Max NPP	extinction age (Ma)
Australopithecus anamensis	0.6	18.9	18.2	718.5	32.5	1010.7	3.85
Australopithecus afarensis	0	16.6	0	904.5	34.4	1310.5	3
Paranthropus boisei	0.1	15.3	93.7	809.4	29.8	968.5	1.3
Paranthropus robustus	1.7	9.2	113	370	26.2	610.6	0.96
Homo habilis	0	11.3	24.4	797.7	30.9	1001.2	1.39
Homo ergaster	0	-4.3	0	732.5	35.9	899	0.88
Homo erectus	0	-22.3	0	1290	33.6	833.4	0.11
Homo heidelbergensis	0	-23.3	0	1069	34.7	873	0.2
Homo neanderthalensis	0	-32.5	0	834.5	31.3	626.2	0.04
Homo sapiens	0	-35.2	0	1050.4	33.4	797.6	0.04

B

Node	descendants	minPrec	minTemp (°C)	Min NPP	maxPrec (mm)	maxTemp (°C)	Max NPP	mean age (Ma)
11	hominins	0.5	17	19.2	736	32.6	1016.6	4.96
12	*Homo* spp.	0.1	-3.7	9.5	854	33.3	912.4	2.87
13	*Homo* spp. without *H. habilis*	0.1	-7.5	6.8	872.6	33.6	891.5	2.34
14	MHS	0	-26.6	1.1	967.1	33.2	786.5	1.03
15	MHS without *H. heidelbergensis*	0	-29.3	0.3	988.9	33.2	778.6	0.49
16	*H. ergaster* plus *H. erectus*	0	-7.7	5.4	870.9	33.9	890.1	1.91
17	australopiths	0.5	17.7	20	733.8	32.5	1024	4.47
18	*Australopithecus* spp.	0.5	17.9	19.1	734.5	32.6	1028.1	4.25
19	*Paranthropus* spp.	0.6	17.2	31.1	722	32	999.7	3.77

Table S4. A. Paleoclimatic estimates for the hominin species in the tree. B. Reconstructed climatic values at the tree nodes after randomly shuffling the fossil occurrence data within the biogeographical domain of individual species. Nodes refer to the node number in the tree. Related to Figures 1 - 3.

A

Species	minPrec (mm)	minTemp (°C)	Min NPP	maxPrec (mm)	maxTemp (°C)	Max NPP	extinction age (Ma)
Australopithecus anamensis	13.4	22.0	48.3	465.3	29.8	431.3	3.85
Australopithecus afarensis	8.5	16.7	73.7	561.7	30.4	699.3	3.00
Paranthropus boisei	5.7	16.6	58.9	877.6	29.6	852.4	1.30
Paranthropus robustus	14.2	9.8	333.9	339.9	24.0	456.6	0.96
Homo habilis	7.7	13.9	22.6	782.6	30.8	848.8	1.39
Homo ergaster	6.0	9.4	0.2	1094.2	33.2	981.9	0.88
Homo erectus	0.6	-15.5	0.0	2000.0	31.2	909.3	0.11
Homo heidelbergensis	0.0	-12.3	0.0	963.3	30.2	1113.7	0.20
Homo neanderthalensis	0.0	-28.2	0.0	586.1	29.2	1093.4	0.04
Homo sapiens	0.0	-33.6	0.0	1105.5	35.6	1458.0	0.04

B

Node	descendants	minPrec	minTemp (°C)	Min NPP	maxPrec (mm)	maxTemp (°C)	Max NPP	mean age (Ma)
11	hominins	12.5	20.0	52.6	513.0	29.9	490.8	4.96
12	*Homo* spp.	6.0	3.8	15.3	946.7	31.5	894.0	2.92
13	*Homo* spp. without *H. habilis*	4.8	0.0	8.8	1032.7	31.8	959.1	2.32
14	MHS	0.7	-21.1	1.7	904.8	31.7	1182.6	0.99
15	MHS without *H. heidelbergensis*	0.2	-23.7	0.5	878.8	31.5	1204.0	0.48
16	*H. ergaster* plus *H. erectus*	4.8	0.7	6.9	1080.7	31.9	960.1	1.91
17	australopiths	12.6	20.5	55.6	499.8	29.8	482.2	4.49
18	*Australopithecus* spp.	12.7	20.8	54.5	492.9	29.8	475.6	4.24
19	*Paranthropus* spp.	12.2	19.7	67.5	522.5	29.5	509.8	3.83

Table S5. A. Paleoclimatic estimates for the hominin species in the tree. B. Reconstructed average climatic values at the tree nodes. Related to Figures 1 - 3.

Transparent Methods

Fossil occurrence and phylogenetic data

The human fossil record dataset we used includes 2,597 hominin occurrences associated with 727 archaeological sites. The time range of our record spans from the first occurrence of australopiths in East Africa dated to some 4.2 Ma, to the definitive advent of *H. sapiens* in Eurasia almost coincident with the demise of *H. neanderthalensis* dated some to 0.040 Ma (see Dataset S1, Raia et al., 2020). We excluded hominin with stratigraphically or geographically restricted fossil record which prevents drawing realistic inference about their climatic niche limits. The species in the database are 2 *Australopithecus* (*A. afarensis* and *A. africanus*), 2 *Paranthropus* (*P. robustus* and *P. boisei*) and 6 *Homo* species (*H. sapiens, H. neanderthalensis, H. heidelbergensis, H. erectus, H. ergaster* and *H. habilis*).

For each fossil occurrence included in the dataset, we recorded paleo-latitude and paleo-longitude, the archaeological layer yielding the remains, and the absolute age of the dated sample. Where available, we also included information about which sample was used for dating the relative lab code. Radiocarbon dates were calibrated using Intcal13 calibration curve for the Northern hemisphere, shcal13 curve for the Southern hemisphere, and marine13 curve for marine samples. Age estimates come with uncertainty. Time averaging of the archaeological layers adds to this uncertainty. To account for this, for each archaeological site (or layer) age estimate we retrieved from the collected estimates the minimum age and the maximum age (calculated according to individual estimates and their respective confidence intervals).

Environmental predictors

Environmental predictors were generated using a paleoclimate emulator (Holden et al., 2019). The method applies Gaussian process emulation of the singular value decomposition of ensembles of runs from the intermediate complexity atmosphere-ocean GCM PLASIM-GENIE with varied boundary-condition forcing (CO_2, orbit and ice-volume). Spatial fields of i) minimum

temperature of the coldest quarter of the year (hereafter, “MinTemp”) , ii) maximum temperature of the warmest quarter (hereafter, “MaxTemp”), iii) minimum precipitation of the driest quarter (hereafter, “MinPrec”), iv) maximum precipitation of the wettest quarter (hereafter, “MaxPrec”), and v) yearly net primary productivity (hereafter, “NPP”) are then emulated at 1,000 year intervals, driven by time-series of scalar boundary-condition forcing, and assuming the climate is in quasi-equilibrium. The emulator uses CO_2 from Antarctic ice cores for the last 800,000 years (Lüthi et al., 2008). Prior to 800 ka, and for the entire sea-level record, it uses the CO_2 and sea-level reconstructions in Stap et al. (2017). Contemporary values of the four bioclimatic variables were derived from WorldClim (Hijmans et al., 2005), while NPP observations were derived from MOD17A3H (MODIS; https://lpdaac.usgs.gov/products/mod17a3hv006/). Current bioclimatic variables and the NPP were interpolated onto the same 0.5° grid and combined with emulated anomalies. Temperature anomalies were additively combined with current temperatures, while precipitation and NPP anomalies were combined with current precipitations using a hybrid additive/multiplicative approach (Holden et al., 2019).

The native-resolution (5°) emulations have been extensively validated (Holden et al., 2019) against model inter-comparisons of the mid-Holocene, the Last Glacial Maximum, the Last Interglacial and the mid-Pliocene warm period. Glacial-interglacial variability was validated (Holden et al., 2019) against observationally based global temperature reconstructions (Köhler et al., 2010). These analyses demonstrated that PALEO-PGEM lies within the uncertainty envelope of high resolution IPCC models, which have themselves been validated against proxy data in the Mid-Holocene and Last Glacial Maximum (Braconnot et al., 2007) and the Pliocene (Haywood et al., 2013). Paleoclimate anomalies at climate model resolution (5°) were downscaled onto the observed modern climatology at 0.5° spatial resolution using bilinear interpolation. We used the entire bioclimatic predictors in order to consider the last 5 million years of human evolution.

Definition of the Climatic Niche limits for *Homo* species

For each hominin species, we built its climatic envelope (the hypervolume defined by the climatic variables), by pooling together all bioclimatic values associated to their fossil occurrences. Then, we selected the recorded minimum values for MinTemp, MinPrec, and NPP, and the maximum values for MaxTemp, MaxPrec, and NPP. We repeated this procedure over 100 replicates. At each replication, the age of each individual archaeological locality was sampled at random from the uniform distribution spanning from the estimated minimum to the estimated maximum locality age. Thus, replication accounts for both ageing uncertainty of individual archaeological layers and, correspondingly, for climatic uncertainty around the paleoclimatic estimates concerning the fossil localities. Finally, for each bioclimatic variable, we took the mean value from each resulting distribution of temperature, precipitation and NPP minima and maxima. Taken together, these mean values of bioclimatic extremes represent a conservative estimate of the climatic range realized for each hominin species during its history, avoiding putting too much faith on extreme values attached to individual replicates and locality.

Definition of the Climatic Niche limits for common ancestors in the hominin tree

The 10 species phylogenetic tree was obtained by combining the Primate (and human) phylogenetic information published in recent papers (Diniz-Filho et al., 2019; Melchionna et al., 2020; Parins-Fukuchi et al., 2019). We started by using the six climatic variables, representing the limits (minima and maxima) in temperature, precipitation and NPP. Since these variables are highly correlated to each other, we reduced covariation among variables by performing a Principal Component Analysis (PCA) on climatic variables associated with each hominin species occurrence in the fossil record. Then, we extracted the PC scores and used them as a multivariate dataset for the phylogenetic ridge regression. To estimate the rates of climatic niche limits evolution we applied the function *RRphylo* (Castiglione et al., 2018) in the R package RRphylo. The function estimates

rates and ancestral states estimates by means of phylogenetic ridge regression. PC scores were used as the response variable in *RRphylo*.

We used the PC scores estimated by *RRphylo* at each node (ancestral states) and back transformed the scores in climatic variables (MinTemp, MinPrec, min NPP, MaxTemp, MaxPrec, max NPP) to map geographically the areas associated with the corresponding climatic estimates (i.e. the area within the limits of the climatic envelope for each ancestor in the tree). The resulting map thus represents the geographic areas estimated to be climatically suitable for occupation by the hominin ancestors. To account for uncertainty around the ages of individual nodes in the hominin phylogeny, we repeated the entire procedure at each node over 100 replicates by using the 100 alternative phylogenies generated from *swapONE* function embedded in the RRphylo package. This function randomly changes the tree topology and branch lengths although it is possible to keep specific clades monophyletic. However, we accounted for a few, well-supported, monophyletic clades which are present in the hominin tree. In particular, in swapping the tree tips and moving (in time) the nodes in the tree, we kept *H. ergaster* and *H. erectus* as sister species. We similarly kept monophyletic the clade subtending to the four australopithecines in the tree, the clade representing the genus *Homo*, and the clade including *H. heidelbergensis*, *H. neanderthalensis* and *H. sapiens*. Since the inclusion of particular taxa in the data may alter significantly the result of PCA ordination (Adams et al., 2011) we repeated the swap procedure leaving one species at random out of the tree for each replicate.

Eventually, for each given species and ancestor in the tree we recorded the number of times a given geographical cell counts as climatically suitable out of the 100 replicates, thus defining an overall 'habitat quality' metric, representing the number of iterations (out of 100) a geographic cell was found habitable (i.e. fell within climatic tolerance limits) for any given species or ancestor in the tree. For each cell, habitat quality thus ranges between 0 (never suitable) to 1 (always suitable).

Measuring the association between the archaeological record and habitat quality

Climatic variables limit at the tree node represent the estimated tolerance limits for hominin ancestors. Since these values are estimated, rather than observed, to assess the association between the position of fossil localities and habitat quality for each ancestral species estimates we selected the fossil occurrences of its descendants, provided they are not included in a descending node which was itself tested. For instance, the EHS ancestor was tested by selecting the fossil occurrence of *H. habilis*, *H. erectus* and *H. ergaster*, but not *H. sapiens*, *H. neanderthalensis* and *H. heidelbergensis* which were considered only descendant to the MHS ancestor. To measure the association between climatic suitability and the presence of human species, we calculated the Area Under receiver-operator Curve (AUC) averaging over the 100 replicates. AUC theoretically ranges from 0 to 1. However, since random sampling points, (pseudoabsences) are not real absences, AUC cannot reach 1 (Jimenez-Valverde, 2012), as the maximum AUC value depends on the actual (unknown) area of distribution of the species. To obtain a null distribution of AUC values and assess significance for the real AUC, for each node in the tree we sampled 100 times as many point occurrences as with the real data (i.e. the fossil occurrences of the species descending from that node) within the biogeographic domain of the species groups (i.e. the descendants to a given node in the tree), and calculated the random AUC. To account for sampling differences between the hominin species, we further repeated the AUC computation after sampling randomly no more than 100 occurrences per species at each replicate.

Measuring rates of climatic niche limits evolution

We used the evolutionary rates provided by *RRphylo* to apply the function *search.shift* (Castiglione et al., 2018) which tests whether individual clades evolved at significantly different rates as compared to the rest of the tree. The function compares the rates attached to each branch descending from a particular node to the rates for the branches of the rest of the tree. The significance for the rate difference is assessed by means of randomization. In the case of

multivariate data, as with this particular study, the multivariate rate is computed as the 2-Norm (Euclidean) vector of the rates of individual variables.

To look for possible evolutionary trends in climatic tolerances over time we used the function *search.trend* (Castiglione et al., 2019) in the *RRphylo* R package. In *search.trend*, evolutionary rates and phenotypes (including the phenotypic estimates at the nodes) are regressed against their age and the resulting slopes compared to slopes randomly generated under the Brownian motion model of evolution, which is a model assuming no temporal trend is present in the data.

Estimating habitat quality under the Brownian motion model of evolution

To estimate and map habitat quality under the assumption that climatic niche limits evolved under a random walk model with constant variance (namely the Brownian motion model of evolution, BM) we estimated climatic niche limits for human ancestors by using the Rphylopars package in R. In Rphylopars, trait values for tree tips with missing data are assessed according to a single rate of evolution calculated for the rest of the tree and data (Bruggeman et al., 2009). Since we found a significant rate shift in niche width referring to the MHS ancestor (node 14) we derived the estimates for both this ancestor (node 14), and the ancestor of *Homo sapiens* and *Homo neanderthalensis* (node 15), pruning the tree of its descendants, and then treating the node as a species with missing data.

Supplemental references

Adams, D.C., Cardini, A., Monteiro, L.R., O'Higgins, P., and Rohlf, F.J. (2011). Morphometrics and phylogenetics: Principal components of shape from cranial modules are neither appropriate nor effective cladistic characters. J. Hum. Evol. *60*, 240–243.

Braconnot, P., Otto-Bliesner, B., Harrison, S., Joussaume, S., Peterchmitt, J-Y., Abe-Ouchi, A., Crucifix, M., Driesschaert, E., Fichefet, Th., Hewitt, C.D., et al. (2007). Results of PMIP2 coupled simulations of the Mid-Holocene and Last Glacial Maximum – Part 1: experiments and large-scale features, Clim. Past *3*, 261– 277.

Bruggeman, J., Heringa, J. and Brandt, B.W. (2009). PhyloPars: estimation of missing parameter values using phylogeny. Nucl. Acid. Res. *37*, W179-W184.

Castiglione, S., Serio, C., Mondanaro, A., Di Febbraro, M., Profico, A., Girardi, G., and Raia, P. (2019). Simultaneous detection of macroevolutionary patterns in phenotypic means and rate of change with and within phylogenetic trees including extinct species. PLoS ONE *14*, e0210101–13.

Castiglione, S., Tesone, G., Piccolo, M., Melchionna, M., Mondanaro, A., Serio, C., Di Febbraro, M., and Raia, P. (2018). A new method for testing evolutionary rate variation and shifts in phenotypic evolution. Meth. Ecol. Evol. *9*, 974–983.

Diniz-Filho, J.A.F., Jardim, L., Mondanaro, A., and Raia, P. (2019). Multiple Components of Phylogenetic Non-stationarity in the Evolution of Brain Size in Fossil Hominins. Evol. Biol. *46*, 47-59.

Haywood, A.M., Hill, D.J., Dolan, A.M., Otto-Bliesner, B.L., Bragg, F., Chan, W.-L., Chandler, M.A., Contoux, C., Dowsett, H.J., Jost, A., et al. (2013). Large-scale features of Pliocene climate: results from the Pliocene Model Intercomparison Project, Clim. Past *9*, 191–209.

Holden, P.B., Edwards, N.R., Rangel, T.F., Pereira, E.B., Tran, G.T., and Wilkinson, R.D. (2019). PALEO-PGEM v1. 0: a statistical emulator of Pliocene–Pleistocene climate. Geoscientific Model Development *12*, 5137-5155.

Jimenez-Valverde, A. (2012). Insights into the area under the receiver operating characteristic curve (AUC) as a discrimination measure in species distribution modelling. Glob. Ecol. Biogeogr. *21*, 498–507.

Köhler, P., Bintanja, R., Fischer, H., Joos, F., Lohmann, G., and Masson-Delmotte, V. (2010). What caused Earth's temperature variations during the last 800,000 years?. Quat. Sci. Rev. *21*, 129-145.

Lüthi, D., Le Floch, M., Bereiter, B., Blunier, T., Barnola, J.-M., Siegenthaler, U., Raynaud, D., Jouzel, J., Fischer, H., Kawamura, K., and Stocker, T.F. (2008). High-resolution carbon dioxide concentration record 650,000–800,000 years before present. Nature *453*, 379–382.

Melchionna, M., Mondanaro, A., Serio, C., Castiglione, S., Di Febbraro, M., Rook, L., Diniz-Filho, J.A.F., Manzi, G., Profico, A., Sansalone, G., and Raia, P. (2020). Macroevolutionary trends of brain mass in Primates. Biol. J. Linn. Soc.*129*, 14–25.

Parins-Fukuchi, C., Greiner, E., MacLatchy, L.M., and Fisher, D.C. (2019). Phylogeny, ancestors, and anagenesis in the hominin fossil record. Paleobiology *45*, 378–393.

Raia, P., Mondanaro, A., Melchionna M., Di Febbraro, M., Diniz-Filho, J.A.F., Rangel, T.F., Holden, P.B., Carotenuto, F., Edwards, N.R., Lima-Ribeiro, M.S., et al. (2020). Past extinctions of *Homo* species coincided with increased vulnerability to climatic change. One Earth in press.

Stap, L.B., Van De Wal, R.S.W., De Boer, B., Bintanja, R., and Lourens, L.J. (2017). The influence of ice sheets on temperature during the past 38 million years inferred from a one-dimensional ice sheet-climate model. Clim. Past *13*, 1243-1257.